

Two Zebrafish Alcohol Dehydrogenases Share Common Ancestry with Mammalian Class I, II, IV, and V Alcohol Dehydrogenase Genes but Have Distinct Functional Characteristics*

Received for publication, February 2, 2004, and in revised form, May 27, 2004
Published, JBC Papers in Press, July 1, 2004, DOI 10.1074/jbc.M401165200

Mark J. Reimers[‡], Mark E. Hahn[§], and Robert L. Tanguay^{‡¶}

From the [‡]Department of Environmental and Molecular Toxicology, Oregon State University, Corvallis, Oregon 97331 and the [§]Biology Department, Woods Hole Oceanographic Institution, Woods Hole, Massachusetts 02543

Ethanol is teratogenic to many vertebrates. We are utilizing zebrafish as a model system to determine whether there is an association between ethanol metabolism and ethanol-mediated developmental toxicity. Here we report the isolation and characterization of two cDNAs encoding zebrafish alcohol dehydrogenases (ADHs). Phylogenetic analysis of these zebrafish ADHs indicates that they share a common ancestor with mammalian class I, II, IV, and V ADHs. The genes encoding these zebrafish ADHs have been named *Adh8a* and *Adh8b* by the nomenclature committee. Both genes were genetically mapped to chromosome 13. The 1450-bp *Adh8a* is 82, 73, 72, and 72% similar at the amino acid level to the Baltic cod ADH8 (previously named ADH1), the human ADH1B2, the mouse ADH1, and the rat ADH1, respectively. Also, the 1484-bp *Adh8b* is 77, 68, 67, and 66% similar at the amino acid level to the Baltic cod ADH8, the human ADH1B2, the mouse ADH1, and the rat ADH1, respectively. ADH8A and ADH8B share 86% amino acid similarity. To characterize the functional properties of ADH8A and ADH8B, recombinant proteins were purified from SF-9 insect cells. Kinetic studies demonstrate that ADH8A metabolizes ethanol, with a V_{\max} of 13.4 nmol/min/mg protein, whereas ADH8B does not metabolize ethanol. The ADH8A K_m for ethanol as a substrate is 0.7 mM. 4-Methyl pyrazole, a classical competitive inhibitor of class I ADH, failed to inhibit ADH8A. ADH8B has the capacity to efficiently biotransform longer chain primary alcohols (≥ 5 carbons) and S-hydroxymethylglutathione, whereas ADH8A does not efficiently metabolize these substrates. Finally, mRNA expression studies indicate that both ADH8A and ADH8B mRNA are expressed during early development and in the adult brain, fin, gill, heart, kidney, muscle, and liver. Together these results indicate that class I-like ADH is conserved in zebrafish, albeit with mixed functional properties.

* This work was supported in part by National Institute on Alcohol Abuse and Alcoholism Grant AA12783 and NIEHS, National Institutes of Health, Grants R01ES06272, ES00210, and ES03850. This is contribution 11165 from the Woods Hole Oceanographic Institution. The costs of publication of this article were defrayed in part by the payment of page charges. This article must therefore be hereby marked "advertisement" in accordance with 18 U.S.C. Section 1734 solely to indicate this fact.

The nucleotide sequence(s) reported in this paper has been submitted to the GenBank™/EBI Data Bank with accession number(s) AF295407 and AY309075.

¶ To whom correspondence should be addressed: Dept. of Environmental and Molecular Toxicology, Oregon State University, 1007 Agriculture and Life Sciences, Corvallis, OR 97331. Tel.: 541-737-6514; Fax: 541-737-7966; E-mail: Robert.Tanguay@oregonstate.edu.

Fetal alcohol syndrome in children born to women who consumed alcohol during pregnancy was first described by Jones and colleagues in 1973 (1). Fetal alcohol syndrome is characterized by a delay in development, cardiac abnormalities (1), central nervous abnormalities, abnormal craniofacial features, and intellectual delays (1, 2). The teratogenic properties of ethanol have been firmly established; however, the underlying mechanism(s) of toxicity remain unclear. Two molecular mechanisms have been proposed: direct ethanol effects and the indirect effects associated with acetaldehyde formation and oxidative stress (3). The ability of ethanol to cause developmental anomalies has been demonstrated in mice, rats, *Drosophila melanogaster*, and chickens (4–7). Zebrafish are well suited for genetic studies (reviewed in Ref. 8). Zebrafish embryos exposed to ethanol display craniofacial abnormalities, cardiac and structural malformations, and development delay (9–11). Visual function was affected in embryos exposed to 1.5% ethanol during development (12). Recent studies indicate that three adult strains of zebrafish display different behaviors in response to ethanol exposure, reflecting underlying genetic differences (13). Whether ethanol metabolism is involved in producing these ethanol-dependent endpoints in zebrafish remains unknown.

Alcohol dehydrogenases (ADHs)¹ metabolize ethanol to acetaldehyde. ADHs are zinc-containing cytosolic enzymes that consist of two ~40-kDa subunits (14). From mammalian studies, several classes of ADHs have been characterized (for nomenclature, see, on the World Wide Web, www.gene.ucl.ac.uk/nomenclature/genefamily/ADH.shtml). Class I ADHs (ADH1) have low K_m values for ethanol and are responsible for the metabolism of ethanol and other small chain alcohols (15, 16). Pyrazole or 4-methyl pyrazole inhibits class I ADHs (15, 17). Class II ADH isozymes (ADH4) have higher K_m values toward ethanol (15, 16) (reviewed in Ref. 14) and tend to metabolize larger aliphatic and aromatic alcohols/aldehydes (reviewed in Refs. 14 and 18). Importantly, ADH4s are less sensitive than class I enzymes to inhibition by pyrazole derivatives (reviewed in Refs. 14 and 18). Class III ADH (ADH5), also known as glutathione-dependent formaldehyde dehydrogenase (reviewed in Refs. 19–21), preferentially metabolize longer chain aliphatic (longer than butanol) and aromatic alcohols; these activities are not inhibited by pyrazole derivatives (19). Class III enzymes cannot be saturated by ethanol (reviewed in Refs. 18). Class IV (ADH7) enzymes have a lower K_m for retinoids and can metabolize ethanol at higher K_m and V_{\max} values than class I (22). Class V and VI ADHs have not been thoroughly investigated for substrate specificity and functionality (23).

¹ The abbreviations used are: ADH, alcohol dehydrogenase; 12-HDDA, 12-hydroxydodecanoic acid; HMGSH, S-hydroxymethylglutathione; 4-MP, 4-methyl pyrazole.

We report here the identification of two zebrafish alcohol dehydrogenases. Based on deduced amino acid sequence analysis, phylogenetic comparisons, genetic mapping, and the metabolic properties of this protein, we have classified ADH8A as a functional zebrafish class I alcohol dehydrogenase. However, ADH8B is classified as a zebrafish class I alcohol dehydrogenase based on phylogenetic analysis, but it does not function as a typical class I enzyme. The zebrafish alcohol dehydrogenase was named in accordance with the HUGO Gene Nomenclature Committee for Gene Family Nomenclature on Alcohol Dehydrogenase and consultations with the Zebrafish Nomenclature Committee. Since these genes are orthologous to multiple mammalian ADH genes, the next available number in the ADH nomenclature scheme, ADH8, was used. We have named these paralogs as *Adh8a* and *Adh8b*.

EXPERIMENTAL PROCEDURES

Materials—NAD, GSH, and 4-methyl pyrazole (4-MP) were purchased from Sigma; semicarbazide, 12-hydroxydodecanoic acid (12-HDDA), 1-hexanol, and 1-octanol were purchased from Aldrich; methanol, 1-propanol, and 1-pentanol, was obtained from Fisher; and 1-butanol was purchased from Acros Organics (Pittsburgh, PA). These reagents were at least 99% pure. Absolute ethyl alcohol USP was purchased from AAPER Alcohol and Chemical Co. (Shelbyville, KY).

Isolation and Sequence Analysis of a cDNA Coding for Zebrafish Alcohol Dehydrogenases—An expressed sequence tag (fb62d02) was acquired through the Incyte IMAGE consortium because of its similarity to previously characterized mammalian alcohol dehydrogenases. The entire cDNA was sequenced and submitted to GenBank™ as accession number AF295407. Another expressed sequence tag (fb23g01) was acquired through Incyte IMAGE consortium based on its similarity to mammalian alcohol dehydrogenases. The entire cDNA was obtained by rapid amplification of cDNA ends, sequenced, and submitted to GenBank™ as accession number AY309075. The deduced amino acid sequences were analyzed and compared with other protein sequences using the National Center for Biotechnology Information data base (available on the World Wide Web at www.ncbi.nlm.nih.gov/BLAST). Class I and III ADH candidates from several species were selected for sequence alignment and comparisons. Multiple sequence alignment and boxshade sequence alignments were performed using two sites on the World Wide Web: the Baylor College of Medicine site (www.hgsc.bcm.tmc.edu/) and ch.EMBnet.org, respectively. The alignments were constructed using the deduced full-length amino acid sequences of various ADH forms from several species (see the figure legends for details).

Phylogenetic Analysis—Multiple sequence alignments were performed using ClustalX, version 1.64b (24). The aligned amino acid sequences were used to construct phylogenetic trees using maximum parsimony and minimum evolution (distance) optimality criteria in PAUP*4.0b10 (25). Alignment positions with gaps were excluded. Maximum parsimony analysis was performed using the branch-and-bound algorithm. For the minimum evolution analysis, mean character difference was used as the distance measure, and the tree-bisection-reconnection algorithm was applied to the starting tree, obtained via the neighbor-joining algorithm. Bootstrap analysis (34) using 100 replicates was performed to assess relative confidence in the topology obtained.

Gene Mapping—The LN54 RH panel, a hybrid between zebrafish and mouse cells, was obtained from Dr. Marc Ekker (Loeb Health Research Institute, Ottawa, Canada). The panel of 94 hybrid DNAs was used to map the *Adh8a* and *Adh8b* chromosomal locations according to described methods (26). In brief, 20- μ l PCRs contained 100 ng of the hybrid cell DNA from each parental cell line, 0.25 μ M of each primer, 50 mM KCl, 0.2 mM each of dNTPs, 10 mM Tris-HCl, pH 8.3, and 1 unit of *Taq* DNA polymerase. PCR was performed with the following conditions for *Adh8a*: 60 s for 94 °C, 90 s for 62 °C, and 90 s for 72 °C for a total of 32 cycles using the ADH8aF1 (5'-GCTCTGTGTGTGCTGTATTC) and ADH8aR2 (5'-GTGCACCTCGATTGAGAAGTC) primers. For *Adh8b*, the conditions used were as follows: 60 s for 94 °C, 90 s for 60 °C, and 90 s for 72 °C using the ADH8bF3 (5'-AAGCCGTCCAGCAGAAAGCAC) and ADH8bR4 (5'-AGAAGCTCAGGAGCGACTCCC) primers. The PCR products were separated on a 2.0% agarose gel and visualized by ethidium bromide staining and UV illumination. This assay was replicated twice before assigning a linkage group (chromosome) number using Dr. Igor Dawid's online mapping program

(NICHD, National Institutes of Health; available on the World Wide Web at mgchd1.nichd.nih.gov:8080/zfrh/beta.cgi).

Zebrafish ADH8A and ADH8B Protein Expression and Purification—The open reading frame of *Adh8a* was subcloned into the Sall and NotI sites, and the *Adh8b* open reading frame was subcloned into the BamHI and HindIII sites of the pBlueBac 4.5 vector (Invitrogen) followed by co-infection of the recombinant baculovirus into SF-9 insect cells. A 500-ml culture for each clone, containing $\sim 600 \times 10^6$ cells, was harvested 48 h postinfection, and cells were pelleted and resuspended in buffer A (100 mM potassium phosphate buffer, pH 7.4, 1 mM EDTA, 1 mM 2-mercaptoethanol, and 0.02% Triton X-100) with a mixture of protease inhibitors, 8 mM phenylmethylsulfonyl fluoride, 1 μ g/ml leupeptin, and 1 μ g/ml pepstatin A, followed by sonication. The homogenates were cleared by centrifugation prior to loading on 4-ml 5'-AMP immobilized agarose (Sigma) affinity columns. ADH8A- and ADH8B-containing extracts were each applied to separate columns followed by 45 ml of buffer A wash, with a column flow rate set at 1 ml/min. The columns were then washed with 45 ml of buffer B (450 mM potassium phosphate buffer, pH 7.4, containing 1 mM EDTA, 1 mM 2-mercaptoethanol, and 0.02% Triton X-100) followed by a 45-ml high stringency wash buffer C (25 mM potassium phosphate buffer, pH 7.4, containing 1 mM EDTA, 1 mM 2-mercaptoethanol, and 0.02% Triton X-100). ADH8A and ADH8B were eluted from their respective columns with buffer C containing 0.25 mM NAD. All fractions were analyzed by 12% SDS-PAGE using ultrasensitive Coomassie Blue stain. The fractions containing either ADH8A or ADH8B were pooled and dialyzed separately against 2 liters of 10 mM Tris-HCl, pH 7.5, 0.1 mM potassium chloride, and 1 mM dithiothreitol at 4 °C followed by a YM-3 Centricon™ concentrating apparatus (Millipore Corp.). Protein concentrations were determined using the Bradford assay (Bio-Rad). Crude cell lysate and purified ADH8A and ADH8B proteins were subsequently analyzed on a gradient SDS-polyacrylamide gel (4–20%) (Bio-Rad) using ultrasensitive Coomassie Blue stain.

Enzyme Kinetics—The enzyme activity assays for the ADHs were performed on the SpectraMax® 90, 96-well plate spectrophotometer (Molecular Devices Corp., Sunnyvale, CA) at 340 nm to measure NADH production over time in a 200- μ l reaction volume. Each well contained 100 mM sodium phosphate buffer, pH 7.4, 5 μ g of ADH8A or ADH8B, 30 mM semicarbazide, and 1 mM NAD. The reaction was initiated with the addition of 20 mM ethanol, 30 mM methanol, 30 mM 1-propanol, 30 mM 1-butanol, 1 mM 1-pentanol, 1 mM 1-hexanol, or 1 mM 1-octanol to measure ADH8A and ADH8B specific activity for each substrate. Reactions utilizing either 1 mM 12-HDDA acid or *S*-hydroxymethylglutathione (HMGSH) that formed spontaneously when 1 mM glutathione was combined with 1 mM formaldehyde also contained in each well 100 mM sodium phosphate buffer, pH 7.4, 5 μ g of ADH8A or ADH8B, and 1 mM NAD. No semicarbazide was added to these wells, since it reacts with aldehydes, thus inhibiting the production of NADH. These specific substrate concentrations have been shown to saturate class III enzymes (19). The reactions were carried out for 10 min at 28 °C to match the normal zebrafish environmental temperature. A blank reaction was run simultaneously without the addition of substrate to correct for any substrate-independent NADH generation.

For the determination of Michaelis-Menten constants for ADH8A and ethanol, the same reaction mixture was used, except the ethanol concentrations were varied between 0.025 and 20 mM. To determine whether this enzyme was inhibited by a pyrazole derivative, from 100 μ M up to 10 mM 4-methyl pyrazole was added 5 min prior to the addition of ethanol 20 mM (final concentration). The 200- μ l reaction contained 100 mM of sodium phosphate buffer, pH 7.4, 5 μ g of ADH8A, 30 mM semicarbazide, and 1 mM NAD.

To determine the Michaelis-Menten constants for ADH8B, the reaction conditions were as stated above; however, concentrations of each of the substrates (pentanol, hexanol, octanol, and HMGSH) were varied between 0.03125 and 10 mM. The glutathione-formaldehyde reaction contained the same reaction mixture except for semicarbazide. The kinetic data were analyzed using SigmaPlot 2001 Enzyme Kinetic module (SPSS Inc., Chicago, IL).

***Adh8a* and *Adh8b* mRNA Expression Levels**—Total RNA was isolated with TRI reagent (Molecular Research Laboratories, Cincinnati, OH) according to the manufacturer's instructions as previously described (27). The reverse transcription reactions were carried out using 2 μ g of total RNA isolated from developmental stages between 24 h postfertilization and 6 days postfertilization. Each RNA sample was isolated from pools consisting of 150 developmentally staged animals. For the adult expression studies, total mRNA was isolated from a whole individual adult, and 1 μ g was used for each tissue expression study. Each 20- μ l reverse transcription reaction contained 1 \times SuperScript™

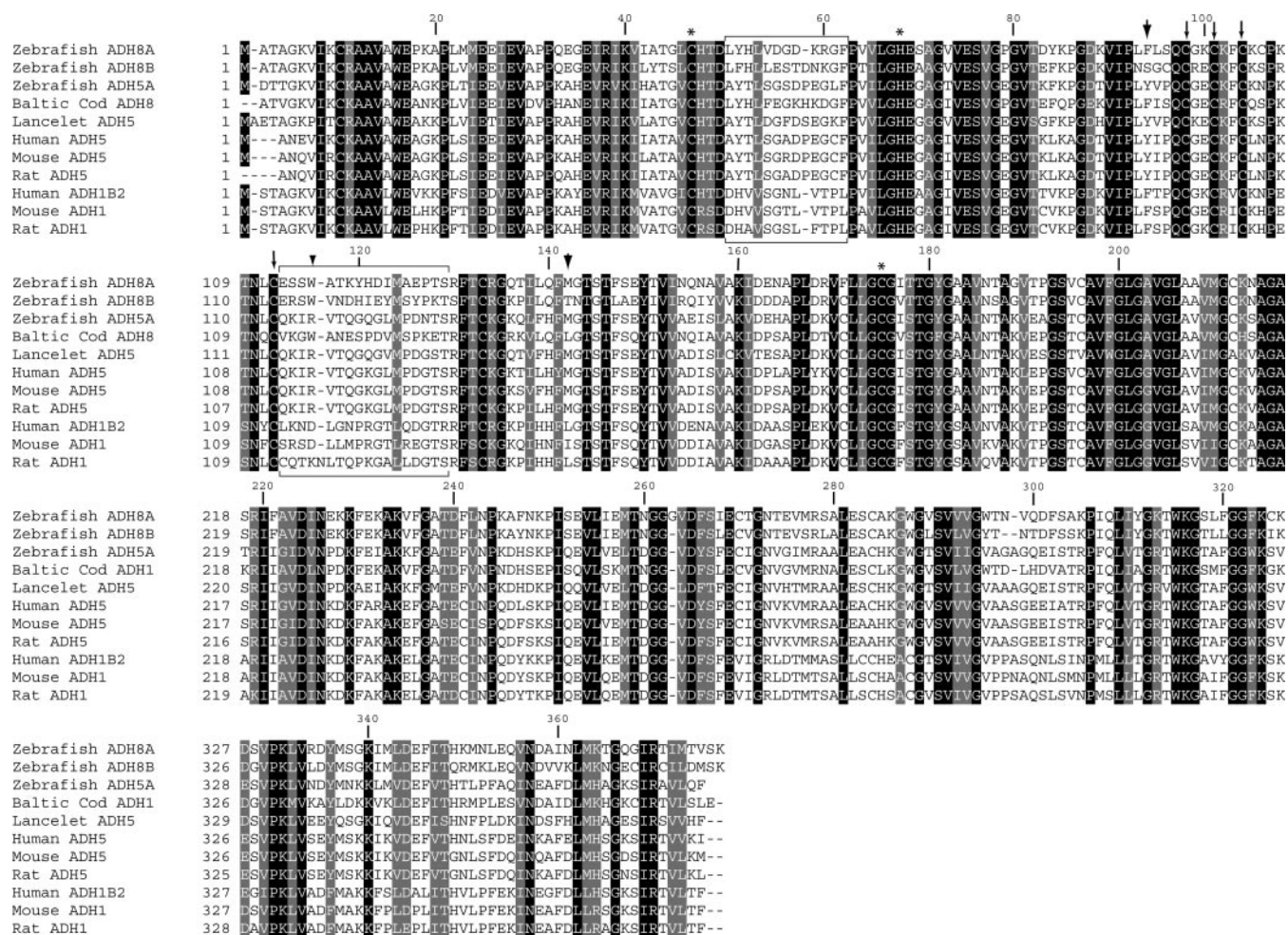


FIG. 1. Predicted amino acid alignment of class I and III ADHs from different species. The predicted amino acid sequences of the reported ADHs were aligned using ClustalW followed by BoxShade (Baylor College of Medicine; available on the World Wide Web at searchlauncher.bcm.tmc.edu). Gray shading denotes sequence similarity, whereas black shading denotes sequence identity. Arrows, noncatalytic zinc binding amino acids; *, catalytic zinc binding amino acids; large arrowheads, 4-methyl pyrazole interaction sites; small arrowhead, fatty acid and HMGSH binding site. Boxed areas, variable regions between classes. Accession numbers are as follows: *Homo sapiens* Class ADH1B, GI5002379; *Mus musculus* ADH1, GI6724311; *Rattus norvegicus* ADH1, GI91930; *H. sapiens* ADH5, GI11496891; *M. musculus* ADH5, GI113409; *R. norvegicus* ADH5, GI113410; *Gadus callarius* ADH1, GI482344; *Danio rerio* ADH8A, GI15428578; *D. rerio* ADH8B, GI32250998; *D. rerio* ADH5A, GI18858257; *Branchiostoma lanceolatum* ADH5, GI8132343.

II First-Strand buffer (50 mM Tris-HCl, pH 8.3, 75 mM KCl, 3 mM MgCl₂), 0.5 mM dNTPs, 250 ng of oligo(dT) primer, 0.01 M dithiothreitol, 40 units of rRNasin® ribonuclease inhibitor, and 200 units of SuperScript™ II reverse transcriptase (Invitrogen). The following components (oligo(dT) primer 15-mer, total RNA, dNTPs, and distilled water) were added to a microcentrifuge tube and heated for 5 min at 65 °C. The contents were centrifuged, and the First-Strand buffer, dithiothreitol, and rRNasin were then added to the above mixture. This reaction was incubated at 42 °C for 2 min, followed by the addition of SuperScript™, and incubated at 42 °C for 50 min and heat inactivation at 70 °C for 15 min. Standard quantitative PCR was conducted. Briefly, each reaction contained 1× DyNamo SYBR Green quantitative PCR kit (containing modified *Thermus brockianus* DNA polymerase, SYBR Green I, optimized PCR buffer, 2.5 mM MgCl₂, dNTPs, Finnzymes; distributed by MJ Research, Inc.) and 0.3 μM forward and reverse primers: ADH8A forward (5'-TCC TCT TCC TCT CTC AGT GTG-3') and reverse (5'-CTT GTA GGT TCA GCC ATA ATG TTA T-3'); ADH8B forward (5'-GAC AGA CAA TAA AGG TTT TCC CAC-3') and reverse (5'-GTT TTG GGA TAT GAC ATA TAT TCA A-3'); β-actin forward (5'-AAG CAG GAG TAC GAT GAG TC-3' and reverse (5'-TGG AGT CCT CAG ATG CAT TG-3'). The reactions were optimized and cycled in a MJ Research® DNA Engine Opticon™ 2 real time system (San Francisco, CA) using the following conditions: 95 °C for 10 min and 94 °C for 10 s, 56 °C for 20 s, and 72 °C for 14 s for a total of 39 cycles. Standard curves were generated with known amounts of target DNA for each target, and each reaction was performed in triplicate. The cycle threshold, or C(t), line was set manually for each of the gene standard curves using the Opticon Monitor™ software (MJ Research). This threshold was auto-

matically applied to wells for consistent analysis of individual samples and standards for the experiments. Agarose gel electrophoresis and thermal denaturing (melt curve analysis) were used to confirm specific gene product formation.

RESULTS

Isolation and Analysis of cDNA Coding for Zebrafish ADH8A and ADH8B—An expressed sequence tag (fb62d02) was acquired through the Incyte IMAGE consortium because of its similarity to alcohol dehydrogenases. The entire cDNA was sequenced and submitted to GenBank™ as accession number AF295407, and we have named it *Adh8a* (see below). This 1450-bp cDNA encodes a predicted 377-amino acid protein (Fig. 1). Another expressed sequence tag (fb23g01) consisting of a partial cDNA clone was acquired through the Incyte IMAGE consortium and appears to be a paralog of *Adh8a*; this cDNA was named *Adh8b* (see below). The entire cDNA was cloned by rapid amplification of cDNA ends, sequenced and submitted to GenBank™ as accession number AY309075. This 1484-bp cDNA encodes a predicted 376-amino acid protein. Both cDNAs encode proteins having a theoretical molecular mass of ~40 kDa (Fig. 1). Class I and III ADH proteins from different species were aligned with the zebrafish ADH8A and ADH8B. Several notable observations are evident in the alignment (Fig. 1). Some regions, such as the residues between 65 and 82, are

TABLE I
Percentage identity (similarity) between class I and 3 ADHs from different species

	Zebrafish ADH8B	Zebrafish ADH5A	Baltic cod ADH8	Amphioxus ADH5	Human ADH5	Mouse ADH5	Rat ADH5	Human ADH1B2	Mouse ADH1	Rat ADH1
	%	%	%	%	%	%	%	%	%	%
Zebrafish ADH8A	77 (86)	61 (77)	68 (82)	60 (75)	62 (77)	61 (77)	63 (77)	56 (73)	57 (72)	57 (73)
Zebrafish ADH8B		56 (71)	64 (77)	56 (71)	56 (72)	56 (71)	57 (71)	52 (68)	52 (67)	51 (66)
Zebrafish ADH5A			63 (78)	78 (88)	81 (91)	81 (90)	81 (90)	62 (76)	61 (76)	62 (77)
Baltic Cod ADH1				60 (74)	62 (76)	62 (76)	63 (76)	55 (71)	57 (73)	56 (72)
Amphioxus ADH5					74 (86)	74 (86)	74 (85)	55 (74)	55 (72)	56 (74)
Human ADH5						92 (97)	93 (96)	63 (78)	63 (78)	63 (79)
Mouse ADH5							96 (98)	62 (78)	63 (78)	63 (79)
Rat ADH5								63 (78)	64 (78)	64 (80)
Human ADH1B2									83 (92)	81 (90)
Mouse ADH1										89 (95)

conserved across classes and species. Amino acids at positions 170–182 and 197–206 are also well conserved. There are, however, certain regions of the proteins that are unique to a class. For instance, at positions 51–53, class I is distinguished by the amino acids aspartic acid, histidine, and valine, whereas the class III proteins have alanine, tyrosine, and tryptophan. The aquatic class I ADHs, zebrafish ADH8A and Baltic cod ADH8, have different amino acids at positions 51–53, leucine, tyrosine, and histidine, respectively (Fig. 1). ADH8B has the amino acids leucine, phenylalanine, and histidine, at positions 51–53, respectively. There are additional conserved residues found only in the three aquatic ADH1 proteins, including proline at position 79, lysine at position 89 (also found in mammalian class I), glutamine at positions 140 and 155, and asparagine at position 260. Overall, the zebrafish ADH8A is 82, 77, and 77% similar at the amino acid level to the Baltic cod ADH8, the human ADH5 (glutathione-dependent formaldehyde dehydrogenase), and the previously identified zebrafish ADH5A clone (28), respectively (Table I). The zebrafish ADH8B amino acid sequence is 77, 72, and 71% similar to the Baltic cod ADH8, the human ADH5, and the zebrafish ADH5A, respectively (Table I). ADH8A and ADH8B share 86% amino acid similarity. Simple multiple sequence alignment is insufficient to classify and name these alcohol dehydrogenases. The zebrafish ADH8A protein is only slightly more closely related to the mammalian (human, mouse, and rat) class III ADHs at 77% similarity than to the class I ADHs (72% similarity) (Table I). ADH8B is 70% similar to class III and 66% similar to class I ADHs. It is important to note, however, that the zebrafish ADH5A is clearly the zebrafish ortholog of the mammalian class III ADH (90% similarity) and will likely have classical class III ADH activity.

To better understand the relationships among zebrafish *Adh8a* and *Adh8b* forms and mammalian ADH sequences, phylogenetic analyses were performed using maximum parsimony and distance (minimum evolution) optimality criteria. Similar results were obtained in both analyses, as illustrated by the minimum evolution tree shown in Fig. 2. The two zebrafish ADH8 sequences formed a monophyletic group with Baltic cod protein originally named as ADH1 (29). For consistency, we will refer to this mixed functional ADH as the Baltic cod ADH8. Together, these three sequences formed a sister group to a clade containing all mammalian ADH1, ADH4, ADH6, and ADH7 proteins. The entire clade of fish ADH8 and mammalian ADH1/4/6/7 proteins was strongly supported (present in parsimony and distance trees and with a distance bootstrap value of 100), and this clade was distinct from the fish and mammalian class III proteins (ADH5). The topology of these trees suggests that zebrafish ADH8A/B and cod ADH8 share a unique common ancestor with the mammalian ADH1, ADH4, ADH6, and ADH7 proteins and that the diversification of these four mammalian ADH classes (I, II, IV, and V) occurred after the divergence of the mammalian and fish lin-

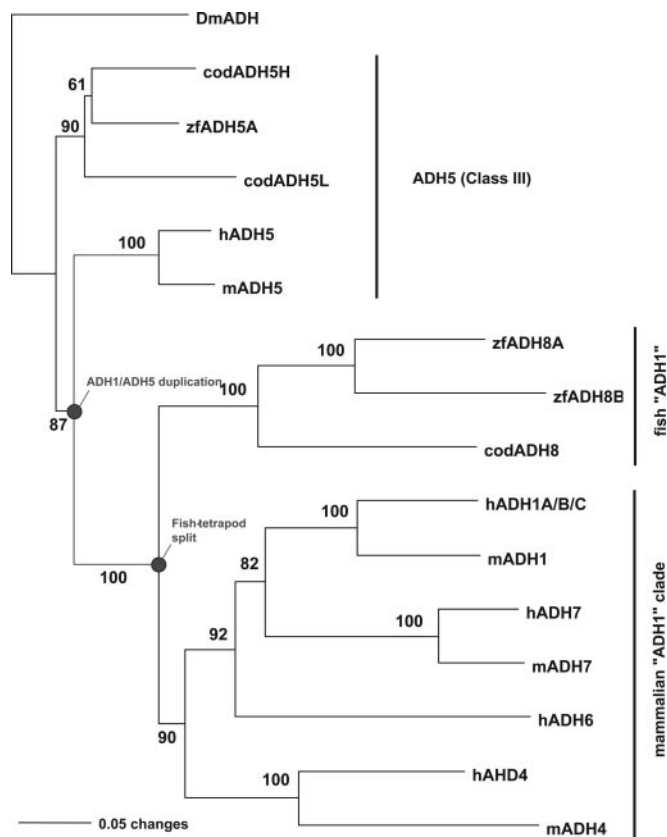


FIG. 2. **Phylogenetic analysis of ADH proteins.** Trees were constructed using minimum evolution (distance) and maximum parsimony as optimality criteria. The distance tree is shown, along with bootstrap values based on 100 resamplings. Accession numbers were the same as those used in Fig. 1 plus the following: *H. sapiens* hADH6, GI4501939; *H. sapiens* hADH4, GI4501935; *H. sapiens* hADH1C, GI4501933; *H. sapiens* hADH1A, GI4501929; *H. sapiens* hADH7, GI4501941; *M. musculus* mADH7, GI5902738; *M. musculus* mADH4, GI6015591; *Gadus morhua* cod ADH5H, GI5902740; *G. morhua* cod ADH5L, GI5902741; *G. callarius* cod ADH8 (formerly cod ADH3_1) Baltic cod mixed functional ADH3/1, GI482344; *D. melanogaster* DmADH, GI17737895.

eages. Because the current system of ADH nomenclature does not provide a way to indicate these co-orthologous relationships, the zebrafish sequences reported here have been assigned the next available family number (family 8).

To determine whether *Adh8a* or *Adh8b* resides on a zebrafish chromosome exhibiting conserved synteny relative to the chromosome containing human ADH genes, *Adh8a* and *Adh8b* gene locations were mapped. A PCR-based approach using the LN54 radiation hybrid panel (a hybrid between zebrafish and mouse cells (26)) was used to map *Adh8a* to chromosome 13, 31.47 centirays from the Z9049 marker. *Adh8b* was

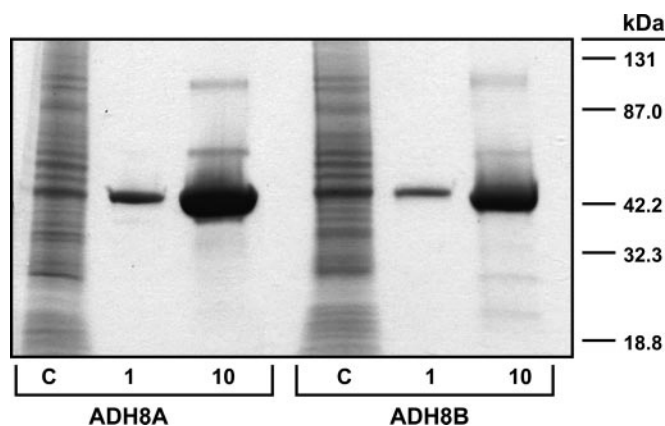


FIG. 3. Recombinantly expressed and purified zebrafish ADH8A and ADH8B proteins. Zebrafish ADH8A and ADH8B proteins resolved on a 4–20% SDS-PAGE gradient stained by Coomassie Blue. The apparent molecular masses of the ADH proteins are 40 kDa. The ADH proteins were purified to near homogeneity (~90% pure). C, crude cell lysate (15 µg of protein); 1, 1 µg of purified ADH8A or ADH8B protein; 10, 10 µg of purified ADH8A or ADH8B protein.

mapped to chromosome 13, 41.25 centirays from Z1627. One centiray is ~148 kb in the LN54 radiation hybrid panel; thus, *Adh8b* is 24.13 centirays or ~3.6 megabases from *Adh8a*. Zebrafish chromosome 13 has a region of conserved synteny with human chromosome 4, the location of all human *ADH* genes. In addition to the LN54 mapping hybrid panel, ADH8A and ADH8B nucleotide sequences were blasted against the zebrafish genome on The Wellcome Trust Sanger Institute site on the World Wide Web (www.ensembl.org/Danio_rerio/), but we were unable to confirm the chromosomal location of these genes as the sequences are not completely represented in the latest genomic data release.

Recombinant Zebrafish ADH8A and ADH8B Protein Purification and Kinetics—Zebrafish ADH8A and ADH8B were recombinantly overexpressed in SF-9 insect cells and were subsequently purified to near homogeneity using a 5'-AMP-agarose affinity chromatography (Fig. 3). Fifteen µg of total protein from crude cell lysates and 1 and 10 µg of purified ADH proteins were resolved by SDS-PAGE followed by sensitive Coomassie Blue staining. The purified proteins were used in subsequent functional studies. First, purified ADH8A protein was used for *in vitro* studies with ethanol as a substrate. The specific activity of this zebrafish ADH8A was 17.9 nmol/min/mg protein for ethanol biotransformation (Fig. 4 and Table II). To determine the ADH8A Michaelis-Menten constants, another ADH8A protein purification was conducted, and ethanol concentrations between 0.025 and 20 mM were used (Fig. 4). The kinetic data for this protein preparation fits a rectangular hyperbola curve ($r^2 = 0.982$) with a calculated V_{\max} of 13.4 nmol/min/mg and a K_m value of 0.7 mM. This K_m value is very similar to those of class I alcohol dehydrogenases (15, 30). However, this alcohol dehydrogenase was not sensitive to 100 µM to 10 mM concentrations of 4-methyl pyrazole, a classic inhibitor of class I alcohol dehydrogenases (Figs. 5 and 6 and Table II). ADH8A specific activity was actually significantly increased with higher concentrations of 4-MP. The specific activity for ADH8A with ethanol alone was 22.7 nmol/min/mg protein, whereas the co-administration of 100 µM, 1 mM, and 10 mM 4-MP was 35.7, 43.8, and 29.2 nmol/min/mg protein, respectively (Fig. 5).

To further characterize the zebrafish ADH8A and ADH8B and to facilitate in the functional classification, specific activities for both enzymes were calculated using several substrates. These substrates were primary alcohols from methanol up to 1-octanol and also 12-HDDA and HMGSH, specific substrates

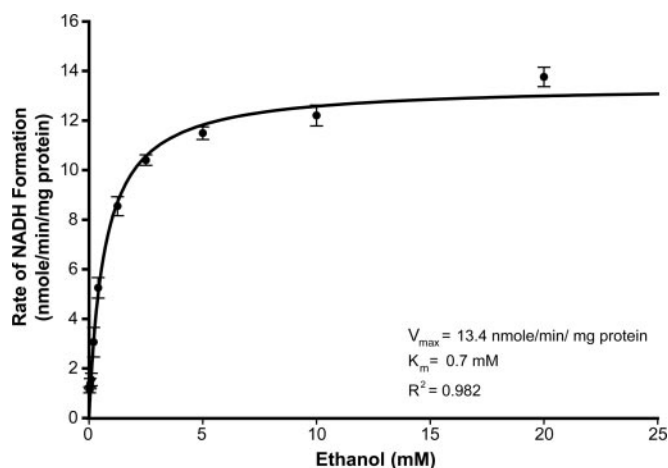


FIG. 4. Zebrafish ADH8A enzyme kinetics using ethanol. The curve fits the Michaelis-Menten kinetics model with $r^2 = 0.982$. The enzyme assay for ADH was performed in a 96-well plate spectrophotometer to measure the production of NADH at 340 nm over time in a 200-µl reaction volume. The reaction was initiated with the addition of various concentrations of ethanol between 0.025 and 20 mM to calculate ADH8A kinetic constants. The reaction was carried out at 28 °C. Shown are mean and S.D. ($n = 3$).

for class III ADHs. ADH8B was unable to metabolize ethanol to acetaldehyde. Both ADH8A and ADH8B failed to metabolize methanol (Fig. 6 and Table II). Further, ADH8A could not convert 1-propanol to its respective aldehyde, whereas ADH8B had minimal activity (3.4 nmol/min/mg protein) toward 1-propanol conversion. Whereas ADH8A effectively metabolizes 1-butanol with a specific activity of 19.5 nmol/min/mg protein, ADH8B only has a nominal specific activity (6.8 nmol/min/mg protein) for 1-butanol. ADH8A has minimal activity toward converting 1-pentanol, 1-hexanol, and 1-octanol to their respective aldehydes with activities of 6.2, 6.3, and 3.6 nmol/min/mg protein, respectively. However, ADH8B efficiently metabolized longer primary alcohols (≥ 5 carbons) as observed with traditional class III ADHs, in particular 1-pentanol, 1-hexanol, and 1-octanol. In addition, HMGSH, a specific substrate for class III ADHs, was efficiently metabolized by ADH8B, whereas there was no detectable activity with ADH8A (Fig. 6 and Table II).

Since ADH8B effectively biotransformed the longer alcohols and HMGSH, Michaelis-Menten constants were ascertained for these substrates. The kinetic data for ADH8B fit rectangular hyperbolas for 1-hexanol ($r^2 = 0.586$), 1-octanol ($r^2 = 0.866$), 1-pentanol ($r^2 = 0.746$), and HMGSH ($r^2 = 0.968$). V_{\max} values of 27.8, 28.8, 22.6, and 30.0 nmol/min/mg protein were measured for 1-hexanol, 1-octanol, 1-pentanol, and HMGSH, respectively (data not shown). The K_m values for hexanol, octanol, pentanol, and HMGSH are 0.04, 0.05, 0.16, and 0.20 mM, respectively (data not shown). ADH8B had minimal activity (7.0 nmol/min/mg protein) with 12-HDDA, whereas ADH8A had a high specific activity (26.8 nmol/min/mg protein) when utilizing 12-HDDA as a substrate (Fig. 6 and Table II). The activities of ADH8A/B for the various substrates are compared in Fig. 6 and Table II.

Temporal and Spatial Expression of Zebrafish *Adh8a* and *Adh8b*—One of the goals is to evaluate the importance of ethanol metabolism on ethanol-mediated developmental toxicity; therefore, it is vital that the temporal and spatial expression pattern of ADH8A and ADH8B are determined. Total RNA was isolated at various developmental stages from 24 h postfertilization to 6 days postfertilization. The RNA was used for quantitative reverse transcription-coupled PCR to monitor ADH8A and ADH8B mRNA expression during zebrafish development (Fig. 7A). Zebrafish ADH8A and ADH8B mRNA were both

TABLE II
Zebrafish ADH8A and ADH8B specific activities using various substrates

Substrate	ADH8A		ADH8B	
	Specific activity	S.D.	Specific activity	S.D.
	<i>nmol/min/mg protein</i>		<i>nmol/min/mg protein</i>	
Ethanol (20 mM)	17.9	1.6	ND ^a	
Ethanol (20 mM) and 4-methyl pyrazole (100 μ M)	23.4	3.6	NA ^b	NA
Methanol (30 mM)	ND		ND	
1-Propanol (30 mM)	ND		3.4	0.23
1-Butanol (30 mM)	19.5	0.74	6.7	0.38
1-Pentanol (1 mM)	6.2	0.79	15.1	0.68
1-Hexanol (1 mM)	6.3	0.85	22.3	0.52
1-Octanol (1 mM)	3.6	0.23	27.9	0.78
12-Hydroxydodecanoic acid (1 mM)	26.8	0.33	7.0	0.05
Glutathione (1 mM)/formaldehyde (1 mM)	ND		27.2	0.12

^a ND, no detection.

^b NA, not applicable.

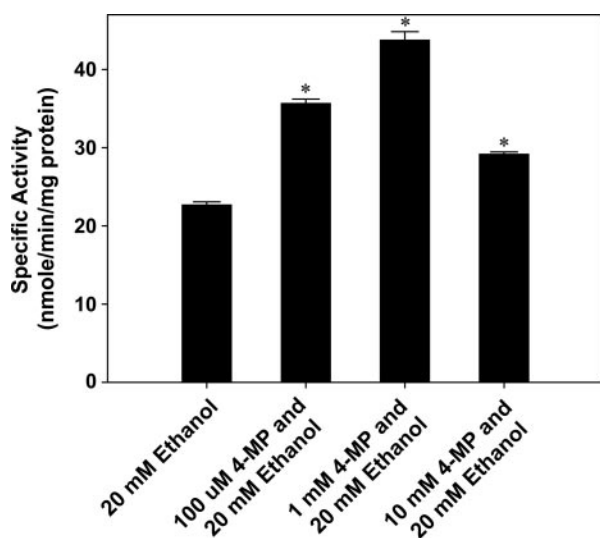


FIG. 5. Competitive inhibition kinetics using 4-methyl pyrazole with zebrafish ADH8A. Saturating concentrations of ethanol (20 mM) were used with varying concentrations of 4-MP (100 μ M, 1 mM, and 10 mM) to inhibit the oxidation of ethanol by ADH8A. ADH8A was incubated with 4-MP for at least 5 min prior to ethanol addition to initiate the reaction. The enzyme assay for ADH was performed in a 96-well plate spectrophotometer to measure the production of NADH at 340 nm over time in a 200- μ l reaction volume. The reaction was carried out at 28 $^{\circ}$ C. Shown are mean and S.E. ($n = 3$).

expressed throughout early life stages of the zebrafish between 24 h postfertilization to 6 days postfertilization. At each early developmental time point, ADH8B mRNA expression was higher than the expression of ADH8A. Furthermore, ADH8B levels were similar across these developmental time points, in contrast to ADH8A, for which mRNA levels increased later in development. Importantly, both transcripts were highly expressed in the RNA isolated from whole adult zebrafish. Assuming that the ADH8A mRNA is translated, these results suggest that the embryo has a limited ability to metabolize ethanol as early as 24 h postfertilization. Zebrafish ADH8A/B-specific antibodies are currently unavailable to confirm this expression pattern.

To determine the adult ADH8A/B mRNA expression pattern, RNA was isolated from several adult tissues for quantitative reverse transcription-coupled PCR analysis. ADH8A and ADH8B mRNAs were expressed in all tissues analyzed, including the brain, fin, gill, heart, kidney, muscle, and liver of the adult zebrafish (Fig. 7B). The highest level of ADH8A expression was in the liver, whereas the lowest levels measured were in the adult caudal fin. ADH8B was moderately expressed in a pattern similar to the ubiquitous expression of class III ADHs in other organisms (31).

DISCUSSION

It has been known since 1971 that ethanol causes developmental effects in zebrafish (10). However, the role of ethanol metabolism in these processes has yet to be determined. Recently a zebrafish alcohol dehydrogenase class III, *Adh5a*, has been described (28); however, the functional properties of the protein are unknown. Here we have identified and characterized two distinct zebrafish alcohol dehydrogenases, which we have named *Adh8a* and *Adh8b*. Alignment of the ADH8 proteins with previously identified ADHs from different species demonstrated that they are \sim 75% similar to both class I and class III ADHs. These differences are distributed throughout the primary sequence (Fig. 1). It is noteworthy that the previously identified zebrafish ADH5A and the human ADH5 are 91% similar in primary sequence, indicating that zebrafish ADH5A is clearly an ortholog of the human ADH5. The genetic mapping studies indicate that zebrafish *Adh8a* and *Adh8b* are both on chromosome 13. Importantly, all of the human ADHs are located on chromosome 4. Genetic mapping studies demonstrate significant conserved synteny between zebrafish chromosome 13 and human chromosome 4. Since *Adh8a* and *Adh8b* are also located on the same chromosome, the genetic mapping does not provide adequate evidence for orthology. It is possible that additional ADH genes will be identified and mapped to chromosome 13.

Our expression studies demonstrate that ADH8A and ADH8B mRNA are developmentally expressed as early as 24 h postfertilization and are expressed in all adult zebrafish tissues examined, including the brain, fin, gill, heart, muscle, and liver. The human ADH5 mRNA is developmentally expressed in the fetal tissues including the brain, lung, liver, and kidney (32). The medium-chain class III alcohol dehydrogenase in *Drosophila melanogaster* is expressed throughout the larval, pupal, and adult life stages of the fly (33). In mice, ADH5 mRNA is detected as early as 6.5 days postcoitum and is nearly ubiquitously expressed in adult tissues (31). ADH1s, on the other hand, have a more restricted tissue-specific expression pattern in the embryo and in adults. In the mouse embryo, ADH1 mRNA expression is detected in the lung at 11.5 days postcoitum and in the kidney and the epithelia of the intestine, bladder, and liver at 16.5 days postcoitum (34). In the adult, ADH1 mRNA is primarily expressed in the liver with extrahepatic expression limited to the kidney, lung, intestine, and stomach mucosa (reviewed in Refs. 31, 32, and 35). The early developmental and primarily adult liver expression of ADH8A mRNA is remarkably similar to the mammalian ADH1. ADH8B mRNA expression more closely resembles mammalian ADH5 expression.

The evolutionary relationship of zebrafish *Adh8a* and *Adh8b* sequences to other mammalian and fish ADHs was inferred

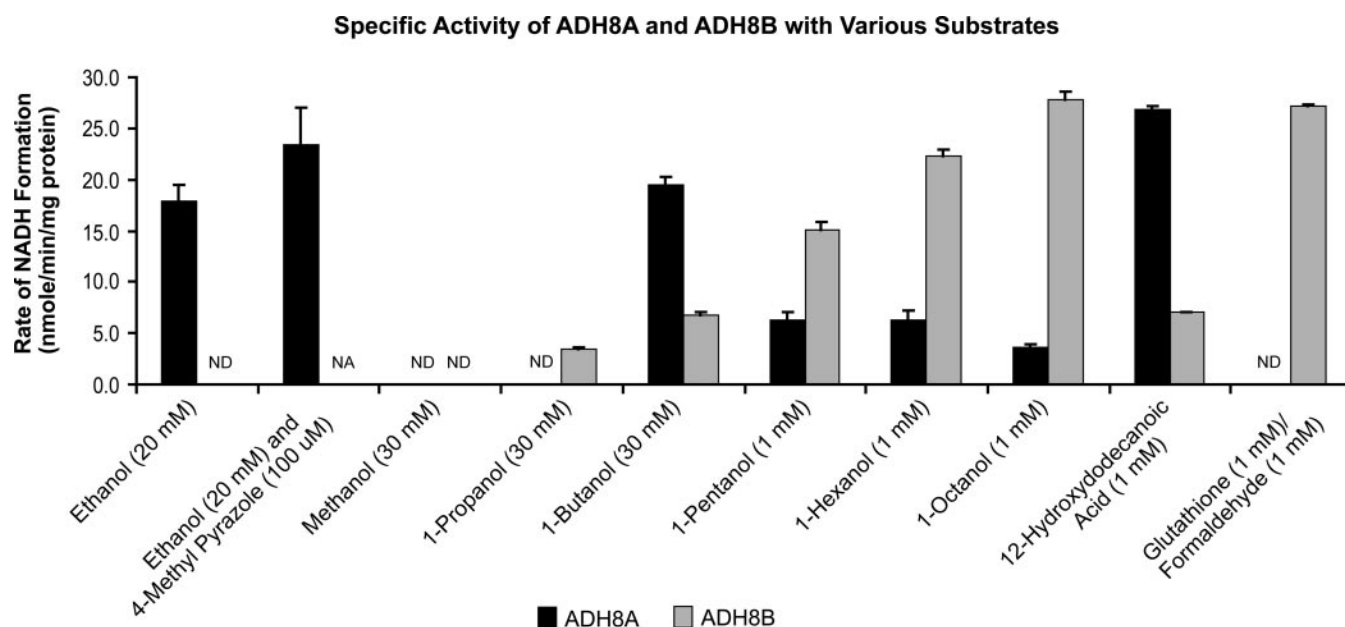


FIG. 6. Zebrafish ADH8A and ADH8B specific activities using multiple substrates. The enzyme assay for ADH was performed in a 96-well plate spectrophotometer to measure the production of NADH at 340 nm over time in a 200- μ l reaction volume. For the alcohol reactions, each well contained 100 mM sodium phosphate buffer, pH 7.4, 5 μ g of ADH8A or ADH8B, 30 mM semicarbazide, and 1 mM NAD. Semicarbazide was excluded in the 12-HDDA and HMGSH reactions. The reactions were initiated with the addition of each of the substrates to calculate their respective ADH8A or ADH8B specific activities. The reaction was carried out at 28 °C. Shown are mean and S.D. ($n = 3$). NA, not applicable; ND, no detectable activity.

using two methods of phylogenetic analysis. Both methods strongly suggested that the zebrafish ADH8 proteins (along with a cod ADH) share a common ancestor with mammalian ADH1, ADH4, ADH6, and ADH7 proteins. If true, this suggests that the most recent common ancestor of mammals and fish possessed two ADH forms: a class III (ADH5) form and a form that was ancestral to extant mammalian class I, II, IV, and V proteins. Cañestro *et al.* (36) estimated the divergence of class I and class III ADH forms to have occurred ~500 million years ago, after the divergence of cephalochordates and vertebrates. Our results support that notion and extend it by providing strong evidence that the divergence of class I and class III ADH forms occurred prior to the divergence of the fish and tetrapod lineages, ~450 million years ago (37). Thus, the gene duplication that led to the class I/class III split probably occurred between 450 and 500 million years ago, in an early chordate.

The date of 450 million years ago also provides an upper bound for the timing of the gene duplications that led to the diversification of mammalian ADH classes I, II, IV, and V. Our analyses and those of others (36, 38) also show that these four classes arose prior to the primate-rodent divergence (65–100 million years ago). Thus, the diversification of ADH classes I, II, IV, and V occurred between 65 and 450 million years ago. This diversification is likely to have resulted from tandem duplications, because these ADH genes are all located in close proximity on the same chromosome in humans (36) and mice (38).

Additional, lineage-specific diversification has occurred within ADH classes. For example, there are three human class I genes, which originated after the rodent-primate split. Similarly, the two zebrafish ADH8 forms appear to have originated after the divergence of the cod and zebrafish lineages. The two zebrafish class I ADH forms may have resulted from a tandem duplication or from the fish-specific genome duplication that is thought to have occurred after the divergence of fish and mammalian lineages (39, 40).

The kinetic data obtained with purified recombinant proteins demonstrate that the zebrafish ADH8A efficiently oxi-

dizes ethanol to acetaldehyde with a K_m of 0.7 mM. This low K_m value is more similar to class I ADHs than class III ADHs, since the latter are not saturated with ethanol up to 2.5 M (41, 42). The K_m values for ADH1s are 2.1 mM and 1.0 mM from human and rat livers, respectively (43). The zebrafish ADH8B fails to metabolize ethanol. Inhibitors are also often used to functionally classify alcohol dehydrogenases. Human and rat ADH1s are inhibited by pyrazole with a K_i of ~50 μ M (43) and 4-MP with a K_i of ~0.5 μ M for the human ADH1 isozymes (reviewed in Ref. 44). Importantly, 4-MP inhibits the Baltic cod ADH8 with a K_i 0.1 μ M (29). Zebrafish ADH8A was not sensitive to concentrations of 4-MP as high as 10 mM. These are novel mixed functional properties for vertebrate ADH enzymes. Based on the kinetics of ethanol metabolism, ADH8A is clearly a class I ADH, but based on inhibition data, ADH8A would be incorrectly classified as a class III enzyme. A recently characterized mixed functional ostrich alcohol dehydrogenase, at the primary sequence level, is most closely related to ADH4s. However, the ostrich ADH is functionally similar to ADH1s with a K_m of 0.7 mM for ethanol and is effectively inhibited by 4-methyl pyrazole (4 μ M) (45). The importance of each of the amino acids inside and outside of the catalytic and coenzyme-binding domains for efficient ethanol metabolism and for pyrazole binding awaits comparative structural studies across alcohol dehydrogenase classes and species.

Zebrafish ADH8B efficiently biotransforms pentanol, hexanol, octanol, and HMGSH. 12-HDDA, a unique substrate for class III ADHs, was minimally metabolized by ADH8B. Since ADH8B was highly effective in metabolizing these substrates, the zebrafish ADH8B protein would be classified as a class III ADH, contrary to phylogenetic analysis classifying it as a class I-like ADH. Thus, the naming of alcohol dehydrogenases based on structural and functional properties should be approached with care until further forms are identified, because the ADHs with mixed functional and phylogenetic affinities represent a nomenclature enigma. Perhaps nomenclature designations should be based solely on evolutionary relationships. These results suggest the possibility that the fish ADH8 proteins

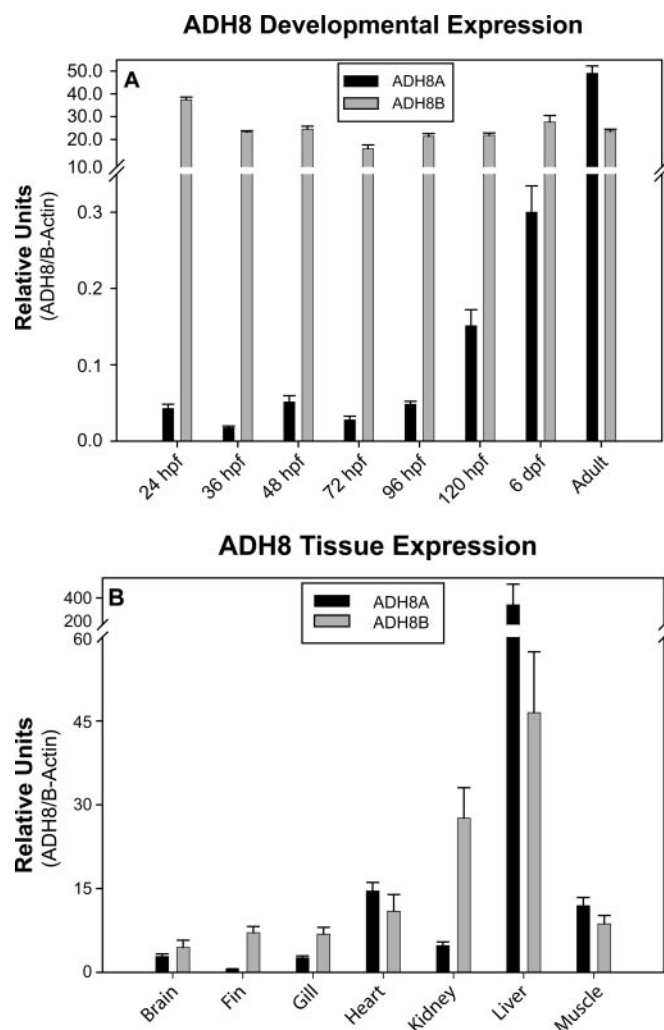


FIG. 7. Developmental and adult organ distribution of zebrafish ADH8A and ADH8B mRNA. Quantitative reverse transcription PCR (*qRT-PCR*) was used to quantify ADH8A and ADH8B mRNA levels. *A*, ADH8A-, ADH8B-, or β -actin-specific primers were used to quantify transcripts in pooled samples isolated at the indicated developmental stages. *B*, the adult tissue distributions of zebrafish ADH8A and ADH8B mRNA were determined from total RNA samples isolated from adult organs. For all quantitative reverse transcription PCRs, ADH mRNA levels were normalized to β -actin levels, and all measurements were conducted in triplicate.

have functional properties like those of an ADH that was ancestral to mammalian class I, II, IV, and V enzymes, providing an evolutionary explanation for the mixed characteristics. If this were the case, the mammalian ADHs may have become more specialized, whereas the fish forms have retained more of the ancestral (mixed) characteristics.

The identification of mixed functional ADHs provides an opportunity to better understand the functional importance of specific amino acids in the enzymes. For example, it is important to understand how ADH8A can be saturated by ethanol yet is not inhibited by 4-MP. Future zebrafish ADH8 structural and mutational analysis is required, but fortunately a significant amount of structural data exists from other species. The x-ray crystallography structure for alcohol dehydrogenase was first determined for horse liver alcohol dehydrogenase (46). The x-ray structure of human ADH1 has also been solved (47). ADHs from other species have also been structurally determined, including the Baltic cod ADH (48). With structural data and computer modeling, functional predictions resulting from amino acid substitutions in substrate specificity, coenzyme

binding affinity, and ethanol oxidation are possible. Based on zebrafish ADH8A and ADH8B primary sequence alignments with class I and III ADHs from other species, the two zinc-binding domains are highly conserved (Fig. 1). The noncatalytic zinc atom interacts with four cysteines at positions 98, 101, 104, and 112 (position numbers relative to zebrafish ADH8A). The catalytic zinc atom interacts with cysteines 47 and 175 and histidine 68. Since there are only three coordinates occupied within the zinc atom, this allows the fourth coordinate to interact with substrates for oxidation and reduction reactions. Adjacent to the catalytic site is the coenzyme-binding domain (reviewed in Ref. 49). Residues in the substrate- and coenzyme-binding domains are of particular interest for describing ADH8A and ADH8B. Table III illustrates a comparison of two classes of ADHs from aquatic and mammalian species. The greatest differences are in the substrate-binding domain compared with the coenzyme-binding pocket. The coenzyme-binding domain is well conserved, $\sim 73\%$ similar, across species and classes. Further, a region of the coenzyme-binding domain is highly conserved at positions 200–206 (Fig. 1). This region has been named the Rossmann fold domain and is found in numerous dinucleotide-binding proteins that utilize FAD, NAD, and NADP (50). The Rossmann dinucleotide-binding domain typically consists of three conserved glycine residues with the sequence GXGXXG. Since alcohol dehydrogenases bind NAD, it is crucial to document the conservation of the Rossmann fold domain in the zebrafish ADHs. The sequence GLGAVG is in both zebrafish ADH8A and ADH8B, which is nearly identical to the human ADH1B2 and ADH5 sequence of GLGGVG.

The substrate-binding pocket has been described and divided into the inner, middle, and outer regions (29). The greater variability of the substrate-binding region may partially explain the mixed functional ADH8A properties. For example, the residues encompassing the substrate-binding site are nearly identical between the human and rat class I ADHs. Similar conservation exists between the human and rat ADH5 substrate pockets (Table III). These substrate-binding residues from the zebrafish ADH8A on average are only 28% identical to the human ADH1 (3 of 11 residues) and surprisingly are also only 28% identical to the human and rat ADH5s. Further, ADH8B has the same percentage identity to the human ADH1 and the two mammalian ADH5s. It is noteworthy that the three aquatic class I ADH proteins are more similar to each other than any of the ADH sequences in the substrate-binding region (7 of 11 residues, or 64%). The residue exchanges that have occurred in ADH8A make the substrate-binding domain more hydrophobic than the human ADH5 and similar in hydrophobicity to the human ADH1. Thus, the structure of ADH8A should have functional properties similar to those of class I ADHs (*i.e.* should metabolize ethanol). These and other specific residue exchanges will probably explain the low ADH8A activity toward longer chain alkyl alcohols and the greater activity toward ethanol.

Specific amino acid exchanges in alcohol dehydrogenases have been used to distinguish between ADH classes. Amino acids at positions 57, 116, 94, and 142 are located in the substrate-binding domain and play a vital role in their interactions with substrates (reviewed in Refs. 51–54). Site-directed mutagenesis studies on Asp⁵⁷, a negatively charged amino acid, was found to be specific and crucial for substrate interactions with class III enzymes (51). Using human ADH5 for site-directed studies, when Asp⁵⁷ was replaced with the class I-specific Leu⁵⁷, there was a marked decrease in HMGSH activity without affecting 12-HDDA enzyme activity (51). The zebrafish ADH8A has Asp⁵⁷, and ADH8B has Thr⁵⁷ (Fig. 1). When the reciprocal experiments were conducted with the hu-

TABLE III
Residues that line the substrate and coenzyme-binding sites of zebrafish ADH8A and ADH8B

Boldface type represents similarity across species' classes.

	Zebrafish ADH8A	Zebrafish ADH8B	Zebrafish ADH5A	Cod ADH8	Human ADH1B2	Rat ADH1	Frog ADH1	Human ADH5	Rat ADH5
Substrate-binding site ^a									
49i	Thr	Thr	Thr	Thr	Thr	Ser	Ser	Thr	Thr
94i	Phe	Ser	Tyr	Phe	Phe	Phe	Phe	Tyr	Tyr
141i	Phe	Phe	Phe	Phe	Phe	Phe	Phe	Tyr	Phe
142i	Met	Thr	Met	Leu	Leu	Leu	Ile	Met	Met
57m	Asp	Thr	Asp	Lys	Leu	Leu	Leu	Asp	Asp
117m	Ala	Val	Val	Ala	Leu	Leu	Ile	Val	Val
296m	Trp	Tyr	Val	Trp	Val	Val	Leu	Val	Val
319m	Leu	Leu	Ala	Met	Val	Ile	Val	Ala	Ala
111o	Leu	Leu	Leu	Gln	Tyr	Leu	Leu	Leu	Leu
307o	Ile	Ile	Arg	Ile	Met	Met	Leu	Phe	Phe
310o	Ile	Ile	Val	Ile	Leu	Leu	Leu	Val	Val
Identities with Zebrafish ADH8A	(11)	7	4	7	3	3	3	3	4
Coenzyme-binding site									
48	His	His	His	His	His	Arg	Arg	His	His
49	Thr	Thr	Thr	Thr	Thr	Ser	Ser	Thr	Ser
52	Tyr	Phe	Tyr	Tyr	His	His	His	Tyr	Tyr
178	Thr	Thr	Ser	Ser	Ser	Ser	Ser	Ser	Ser
205	Gly	Gly	Gly	Gly	Gly	Gly	Gly	Gly	Gly
224	Asp	Asp	Asp	Asp	Asp	Asp	Asp	Asp	Asp
225	Ile	Ile	Val	Leu	Ile	Ile	Leu	Ile	Ile
229	Lys	Lys	Lys	Lys	Lys	Lys	Lys	Lys	Lys
271	Thr	Val	Ile	Val	Ile	Ile	Ile	Ile	Ile
273	Asn	Asn	Asn	Asn	Arg	Arg	Asn	Asn	Asn
370	Arg	Arg	Arg	Arg	Arg	Arg	Arg	Arg	Arg
Identities with Zebrafish ADH8A	(11)	9	8	8	7	5	5	9	8

^a Substrate-binding pocket: i, inner; m, middle; o, outer.

man class I ADH at position 57 (and 116), creating class 3-like Asp⁵⁷ and Arg¹¹⁶, this mutated enzyme had a higher affinity for 12-HDDA and decreased ethanol affinity (54). As a result of these observations, zebrafish ADH8A may have an active site similar to class I ADHs, since it can efficiently oxidize ethanol, but the active binding site has favorable conditions for 12-HDDA binding such as Asp⁵⁷. On the other hand, ADH8B may have a larger active binding site, because it prefers longer chain alcohols and HMGSH. The substrate-binding domain must be large enough for the appropriate HMGSH interactions to occur in ADH8B.

4-MP inhibits class I ADHs at very low concentrations but minimally inhibits class III ADHs. This has been credited to the size of the substrate-binding domain of class III as well as the domain being occupied by charged amino acid residues (reviewed in Ref. 51). 4-MP interacts with positions 94 (54) and 142 (55). Class I ADHs have Phe⁹⁴ and Leu¹⁴², whereas the class III enzymes have Tyr⁹⁴ and Met¹⁴². The importance of position 142 for inhibitor sensitivity has been further evaluated for the mammalian ADH1 and ADH7 enzymes. The human ADH1B1 and class IV ADH (ADH7) exhibit different topological features within the substrate-binding pockets due to a number residue exchanges, causing affinity differences for 4-MP (55). Human ADH7 has a 580-fold lower affinity 4-MP than human ADH1B1 isozyme. The lower affinity was attributed to the distorted covalent bond angles of ADH7 between the pyrazole ring and the enzyme caused by the different position of the nicotinamide ring (55). Structural comparisons indicated that the side chain of Met¹⁴² might interfere with 4-MP docking, causing human ADH7 to have a lower affinity for 4-MP. When the ADH7 Met¹⁴² was changed to Leu, the residue present in ADH1s at position 142, the K_i for 4-MP decreased from 350 to 10 μ M (56). Cumulatively, these results provide a potential explanation for why the zebrafish ADH8A is not sensitive to 4-MP (Met¹⁴²) and the cod ADH8 is inhibited (Leu¹⁴²). Im-

portantly, nearly all class I ADHs have Leu or Ile at this position (Table III). All known class III ADHs have Met at this position. Structural and mutational studies of ADH8A will provide a more thorough understanding of the properties of this enzyme.

In summary, two class I zebrafish alcohol dehydrogenases, ADH8A and ADH8B, were identified and characterized. ADH8A has mixed functional properties, since it has a high affinity for ethanol but was not inhibited by 4-methyl pyrazole. ADH8B, however, had functional properties similar to those of class III ADHs, but through phylogenetic analysis, the protein was classified by as a class I. These mixed functional proteins will provide the basis for rational site-directed mutagenesis and functional studies to better understand the evolution of structure and function of vertebrate alcohol dehydrogenases. The identification and characterization of a zebrafish class I ADH provides an opportunity to determine the importance of these enzymes in normal development and in ethanol-mediated developmental toxicity.

Acknowledgments—We thank Dr. Dennis Petersen for the use of the SpectraMax® 90 96-well plate spectrophotometer and Dr. Marc Ekker (Loeb Health Research Institute, Ottawa, Canada) for supplying the radiation hybrid DNA panel for mapping the Adh8 genes.

REFERENCES

- Jones, K. L., and Smith, D. W. (1973) *Lancet* **2**, 999–1001
- Henderson, G. I., Chen, J. J., and Schenker, S. (1999) *Front. Biosci.* **4**, D541–550
- Reynolds, J. D., and Brien, J. F. (1995) *Can. J. Physiol. Pharmacol.* **73**, 1209–1223
- Becker, H. C., Diaz-Granados, J. L., and Randall, C. L. (1996) *Pharmacol. Biochem. Behav.* **55**, 501–513
- Pierce, D. R., Goodlett, C. R., and West, J. R. (1989) *Teratology* **40**, 113–126
- Bupp Becker, S. R., and Shibley, I. A., Jr. (1998) *Alcohol Alcohol* **33**, 457–464
- Ranganathan, S., Davis, D. G., and Hood, R. D. (1987) *Teratology* **36**, 45–49
- Granato, M., and Nusslein-Volhard, C. (1996) *Curr. Opin. Genet. Dev.* **6**, 461–468
- Reimers, M. J., Flockton, A. M., and Tanguay, R. L. (2004) *Neurotoxicol. Teratol.*, in press

10. Laale, H. W. (1971) *J. Exp. Zool.* **177**, 51–64
11. Blader, P., and Strahle, U. (1998) *Dev. Biol.* **201**, 185–201
12. Bilotta, J., Saszik, S., Givin, C. M., Hardesty, H. R., and Sutherland, S. E. (2002) *Neurotoxicol. Teratol.* **24**, 759–766
13. Dlugos, C. A., and Rabin, R. A. (2003) *Pharmacol. Biochem. Behav.* **74**, 471–480
14. Agarwal, D. P., and Goedde, H. W. (1990) *Pharmacol. Ther.* **45**, 69–83
15. Crabb, D. W., Bosron, W. F., and Li, T. K. (1987) *Pharmacol. Ther.* **34**, 59–73
16. Boleda, M. D., Julia, P., Moreno, A., and Pares, X. (1989) *Arch. Biochem. Biophys.* **274**, 74–81
17. McMartin, K. E., and Collins, T. D. (1988) *J. Toxicol. Clin. Toxicol.* **26**, 451–466
18. Agarwal, D. P. (2001) *Pathol. Biol. (Paris)* **49**, 703–709
19. Koivusalo, M., Baumann, M., and Uotila, L. (1989) *FEBS Lett.* **257**, 105–109
20. Danielsson, O., and Jornvall, H. (1992) *Proc. Natl. Acad. Sci. U. S. A.* **89**, 9247–9251
21. Duester, G., Farres, J., Felder, M. R., Holmes, R. S., Hoog, J. O., Pares, X., Plapp, B. V., Yin, S. J., and Jornvall, H. (1999) *Biochem. Pharmacol.* **58**, 389–395
22. Duester, G. (2000) *Eur. J. Biochem.* **267**, 4315–4324
23. Hoog, J., Brandt, M., Hedberg, J. J., and Stromberg, P. (2001) *Chem. Biol. Interact.* **130**, 395–404
24. Thompson, J. D., Gibson, T. J., Plewniak, F., Jeanmougin, F., and Higgins, D. G. (1997) *Nucleic Acids Res.* **25**, 4876–4882
25. Swofford, D. L. (1998) *PAUP*: Phylogenetic Analysis Using Parsimony (*and Other Methods)*, version 4, Sinauer Associates, Sunderland, MA
26. Hukriede, N. A., Joly, L., Tsang, M., Miles, J., Tellis, P., Epstein, J. A., Barbazuk, W. B., Li, F. N., Paw, B., Postlethwait, J. H., Hudson, T. J., Zon, L. I., McPherson, J. D., Chevrette, M., Dawid, I. B., Johnson, S. L., and Ekker, M. (1999) *Proc. Natl. Acad. Sci. U. S. A.* **96**, 9745–9750
27. Tanguay, R. L., Andreassen, E. A., Heideman, W., and Peterson, R. E. (2000) *Biochim. Biophys. Acta* **1494**, 117–128
28. Dasmahapatra, A. K., Doucet, H. L., Bhattacharyya, C., and Carvan, M. J., III (2001) *Biochem. Biophys. Res. Commun.* **286**, 1082–1086
29. Danielsson, O., Eklund, H., and Jornvall, H. (1992) *Biochemistry* **31**, 3751–3759
30. Hoog, J. O., Vagelopoulos, N., Yip, P. K., Keung, W. M., and Jornvall, H. (1993) *Eur. J. Biochem.* **213**, 31–38
31. Haselbeck, R. J., and Duester, G. (1997) *Alcohol Clin. Exp. Res.* **21**, 1484–1490
32. Estonius, M., Svensson, S., and Hoog, J. O. (1996) *FEBS Lett.* **397**, 338–342
33. Danielsson, O., Atrian, S., Luque, T., Hjelmqvist, L., Gonzalez-Duarte, R., and Jornvall, H. (1994) *Proc. Natl. Acad. Sci. U. S. A.* **91**, 4980–4984
34. Ang, H. L., Deltour, L., Zgombic-Knight, M., Wagner, M. A., and Duester, G. (1996) *Alcohol Clin. Exp. Res.* **20**, 1050–1064
35. Edenberg, H. J., and Bosron, W. F. (1997) in *Comprehensive Toxicology* (Sipes, I. G., McQueen, C. A., and Gandolfi, A. J., eds) Vol. 3, pp. 119–131, Cambridge University Press, Cambridge, UK
36. Canestro, C., Albalat, R., Hjelmqvist, L., Godoy, L., Jornvall, H., and Gonzalez-Duarte, R. (2002) *J. Mol. Evol.* **54**, 81–89
37. Kumar, S., and Hedges, S. B. (1998) *Nature* **392**, 917–920
38. Szalai, G., Duester, G., Friedman, R., Jia, H., Lin, S., Roe, B. A., and Felder, M. R. (2002) *Eur. J. Biochem.* **269**, 224–232
39. Amores, A., Force, A., Yan, Y. L., Joly, L., Amemiya, C., Fritz, A., Ho, R. K., Langeland, J., Prince, V., Wang, Y. L., Westerfield, M., Ekker, M., and Postlethwait, J. H. (1998) *Science* **282**, 1711–1714
40. Taylor, J. S., Van de Peer, Y., Braasch, L., and Meyer, A. (2001) *Philos. Trans. R. Soc. Lond. B Biol. Sci.* **356**, 1661–1679
41. Pares, X., and Vallee, B. L. (1981) *Biochem. Biophys. Res. Commun.* **98**, 122–130
42. Wagner, F. W., Pares, X., Holmquist, B., and Vallee, B. L. (1984) *Biochemistry* **23**, 2193–2199
43. Zorzano, A., and Herrera, E. (1990) *Gen. Pharmacol.* **21**, 697–702
44. Yin, S. J., Han, C. L., Lee, A. I., and Wu, C. W. (1999) *Adv. Exp. Med. Biol.* **463**, 265–274
45. Hjelmqvist, L., Estonius, M., and Jornvall, H. (1995) *Proc. Natl. Acad. Sci. U. S. A.* **92**, 10904–10908
46. Eklund, H., Nordstrom, B., Zeppezauer, E., Soderlund, G., Ohlsson, I., Boiwe, T., Soderberg, B. O., Tapia, O., Branden, C. I., and Akeson, A. (1976) *J. Mol. Biol.* **102**, 27–59
47. Hurley, T. D., Bosron, W. F., Hamilton, J. A., and Amzel, L. M. (1991) *Proc. Natl. Acad. Sci. U. S. A.* **88**, 8149–8153
48. Ramaswamy, S., el-Ahmad, M., Danielsson, O., Jornvall, H., and Eklund, H. (1994) *FEBS Lett.* **350**, 122–124
49. Sytkowski, A. J., and Vallee, B. L. (1979) in *Biochemistry and Pharmacology of Ethanol* (Majchrowicz, E., and Noble, E. P., eds) Vol. 1, pp. 43–63, Plenum Press, New York
50. Bottoms, C. A., Smith, P. E., and Tanner, J. J. (2002) *Protein Sci.* **11**, 2125–2137
51. Estonius, M., Hoog, J. O., Danielsson, O., and Jornvall, H. (1994) *Biochemistry* **33**, 15080–15085
52. Engeland, K., Hoog, J. O., Holmquist, B., Estonius, M., Jornvall, H., and Vallee, B. L. (1993) *Proc. Natl. Acad. Sci. U. S. A.* **90**, 2491–2494
53. Holmquist, B., Moulis, J. M., Engeland, K., and Vallee, B. L. (1993) *Biochemistry* **32**, 5139–5144
54. Hedberg, J. J., Stromberg, P., and Hoog, J. O. (1998) *FEBS Lett.* **436**, 67–70
55. Xie, P., Parsons, S. H., Speckhard, D. C., Bosron, W. F., and Hurley, T. D. (1997) *J. Biol. Chem.* **272**, 18558–18563
56. Xie, P. T., and Hurley, T. D. (1999) *Protein Sci.* **8**, 2639–2644